Neuropsychologia xxx (xxxx) xxx–xxx

Contents lists available at ScienceDirect

Neuropsychologia

journal homepage: www.elsevier.com/locate/neuropsychologia

# Plasticity of the human visual brain after an early cortical lesion

K. Mikellidou[a], R. Arrighi[b], G. Aghakhanyan[a], F. Tinelli[c], F. Frijia[d], S. Crespi[e,f,g], F. De Masi[h], D. Montanaro[i], M.C. Morrone[a,c,*]

[a] Department of Translational Research on New Technologies in Medicine and Surgery, University of Pisa, Pisa, Italy
[b] Department of Neuroscience, Psychology, Pharmacology and Child Health, University of Florence, Florence, Italy
[c] Department of Developmental Neuroscience, Stella Maris Scientific Institute, Pisa, Italy
[d] UOC Bioingegneria e Ingegneria Clinica, Fondazione CNR/Regione Toscana G. Monasterio, Pisa, Italy
[e] Department of Psychology, Vita-Salute San Raffaele University, Milan, Italy
[f] Unit of Experimental Psychology, Division of Neuroscience, Scientific Institute San Raffaele, Milan, Italy
[g] Neuroradiology Unit – CERMAC, San Raffaele Hospital, Milan, Italy
[h] Division of Anesthesiology and Intensive Care, University Hospital of Pisa, Italy
[i] Unità di Neuroradiologia, Fondazione CNR/Regione Toscana G. Monasterio, Pisa, Italy

ARTICLE INFO

*Keywords:*
Visual cortex
Hemianopia
Retinotopic map
pRF
Neural plasticity
Cortical reorganization
Early brain lesion
fMRI
DTI
Contrast sensitivity

ABSTRACT

In adults, partial damage to V1 or optic radiations abolishes perception in the corresponding part of the visual field, causing a scotoma. However, it is widely accepted that the developing cortex has superior capacities to reorganize following an early lesion to endorse adaptive plasticity. Here we report a single patient case (G.S.) with near normal central field vision despite a massive unilateral lesion to the optic radiations acquired early in life. The patient underwent surgical removal of a right hemisphere parieto-temporal-occipital atypical choroid plexus papilloma of the right lateral ventricle at four months of age, which presumably altered the visual pathways during *in utero* development. Both the tumor and surgery severely compromised the optic radiations. Residual vision of G.S. was tested psychophysically when the patient was 7 years old. We found a close-to-normal visual acuity and contrast sensitivity within the central 25° and a great impairment in form and contrast vision in the far periphery (40–50°) of the left visual hemifield. BOLD response to full field luminance flicker was recorded from the primary visual cortex (V1) and in a region in the residual temporal-occipital region, presumably corresponding to the middle temporal complex (MT+), of the lesioned (right) hemisphere. A population receptive field analysis of the BOLD responses to contrast modulated stimuli revealed a retinotopic organization just for the MT+ region but not for the calcarine regions. Interestingly, consistent islands of ipsilateral activity were found in MT+ and in the parieto-occipital sulcus (POS) of the intact hemisphere. Probabilistic tractography revealed that optic radiations between LGN and V1 were very sparse in the lesioned hemisphere consistently with the post-surgery cerebral resection, while normal in the intact hemisphere. On the other hand, strong structural connections between MT+ and LGN were found in the lesioned hemisphere, while the equivalent tract in the spared hemisphere showed minimal structural connectivity. These results suggest that during development of the pathological brain, abnormal thalamic projections can lead to functional cortical changes, which may mediate functional recovery of vision.

## 1. Introduction

The brain has a higher level of cortical plasticity during the first stages of development. As first suggested by Paul Broca back in 1865 (Berker et al., 1986), recovery from brain damage is more frequent when lesions occur perinatally or during the first months of life (see Guzzetta et al., 2010; Werth, 2008 for review). Early-onset of large unilateral lesions to the motor cortex trigger a massive reorganization of the primary motor region and subcortical pathways leading to the abnormal generation of bilateral processing of motor pattern in the undamaged hemisphere (Carr et al., 1993; Kuhnke et al., 2008; Wilke et al., 2009). Similar reorganization has been observed in the developing visual system following early or congenital brain damage of the visual pathways. An example is patient M.S. who had a perinatal bilateral lesion of a major part of Brodmann areas 17 and 18, corresponding to areas V1, V2 and V3 as revealed by Magnetic Resonance Imaging –MRI (Kiper et al., 2002). Patient M.S. was born prematurely at 30 weeks of gestation, suffering a focal ischemic damage secondary to

* Corresponding author at: Department of Translational Research on New Technologies in Medicine and Surgery, University of Pisa, Pisa, Italy.
*E-mail address:* concetta@in.cnr.it (M.C. Morrone).

http://dx.doi.org/10.1016/j.neuropsychologia.2017.10.033
Received 11 July 2017; Received in revised form 16 October 2017; Accepted 29 October 2017

bacterial meningitis at around the time of birth. Despite these profound lesions, M.S. showed slightly reduced contrast sensitivity, a visual acuity around 10 c/deg, and near normal sensitivity for moving stimuli.

Similarly, Amicuzi et al. (2006) reported the case of a 4.5-year-oldpatient (I.S.) born prematurely with a complete bilateral loss of the striate cortex and a portion of the extrastriate cortex. Despite the massive brain lesion, visual acuity and contrast sensitivity of patient G.S. were compromised but not in a severe way. Another example is patient F.O. who had a close-to-normal visual field perimetry despite early unilateral loss of the occipital lobe (Werth, 2006). The authors speculated that residual vision was possibly mediated by intact extrastriate such as MT+ and the lateral occipital complex (LOC) in the damaged cerebral hemisphere. All these single case studies suggest that bilateral and unilateral damage at birth in early visual areas can trigger a massive reorganization of cortical and subcortical pathways, with extrastriate areas mediating the residual visual function.

This view is consistent with the interesting patient studied by Giaschi et al. (2003) who had sparing of the extrastriate cortex, including MT+, while both striate cortices were completely lesioned. The patient had conscious motion perception (Riddoch's phenomenon) that was mediated by a more extensive cortical network of occipital extrastriate areas than those observed in typical subjects (Cardin and Smith, 2010; Morrone et al., 2000; Singh et al., 2000; Smith et al., 1998; Tootell et al., 1997; Zeki et al., 1991). These results suggest that in the absence of striate cortex, the specialization of extrastriate cortex can change and assume different visual functions than those usually observed in the healthy brain. Also sub-cortical visual pathways can be dramatically re-routed in congenital brain lesion patients (Muckli et al., 2009). Despite the lack of an entire cerebral hemisphere, whose development terminated precociously at around the 7th week of gestation, the 10-year-old girl had close-to-normal residual vision in the hemifield contralateral to the lesion (Muckli et al., 2009). Functional MRI (fMRI) revealed that the primary visual area of the left (intact) hemisphere maps both hemifields, with islands of ipsilateral visual field representations within the retinotopic map of the contralateral field. The most likely explanation to account for these results is a re-routing of the fibers crossing at the level of the optic chiasm: axons from both nasal and temporal retina project to the ipsilateral thalamic lateral geniculate nucleus (LGN) and then to the striate cortex.

All the cases discussed above demonstrate that conscious visual processing can survive massive brain lesions, including those to the calcarine cortex either unilaterally or bilaterally. However, *blindsight* patients provide clear-cut evidence on how calcarine cortical lesions are not always accompanied by awareness. Blindsight patients are typically unaware of stimuli presented within their blind field, but are able to perform above chance in psychophysical forced-choice tasks for stimuli presented there, despite damage to the corresponding regions in V1 (Cowey, 2010; Cowey and Stoerig, 1991; Stoerig and Cowey, 2007; for review see Tamietto and Morrone, 2016; Weiskrantz, 1986; Weiskrantz et al., 1974). Blindsight patients show a clear capacity to process 'dorsal' visual stream properties, such as luminance contrast, flicker and motion, leading to the idea that a direct projection from subcortical structures to the extrastriate middle temporal area (MT+) might sustain residual visual functions (Ajina et al., 2015b). Indeed, blindsight patient G.Y., whose left V1 is totally destroyed, has a strong ipsilateral connection between LGN and MT+ (Bridge et al., 2008). Interestingly, the individual strength variation of the direct LGN - MT+ pathway correlates with the probability of blindsight in patients acquiring a striate cortex lesion in adulthood (Ajina et al., 2015b).

The developing infant brain refines major projections and pathways during the first few months of life, and some pruning may take place also in sub-cortical visual pathways (Bourne and Morrone, 2017; Cowey et al., 1994; Nakagawa and Tanaka, 1984; Warner et al., 2010, 2012, 2015). Cortical visual areas may have different developmental time and MT+ develops fine motion properties before V1, suggesting an important role of MT+ in mediating cortical re-routing (for review see Atkinson, 2017; Biagi et al., 2015; Bourne and Rosa, 2006). Interestingly, patients suffering from brain lesions early in life are more likely to develop residual unconscious visual perception (Ptito and Leh, 2007). Tinelli et al. (2013) recently showed that presence of blindsight in patients with congenital, but not acquired, V1 lesion is extraordinary high: all four congenital patients tested performed very well several tasks such as motion direction, orientation or position discrimination amongst hemifields although being unaware of stimuli presented within their blind field (Tinelli et al., 2013). The congenital subjects also show a strong BOLD representation of the ipsilateral visual field in the calcarine cortex, suggesting that early brain lesions can trigger a rewiring of V1 and not just of the extrastriate areas as previously suggested (Bittar et al., 1999).

At present it is not clear why some patients with congenital lesions show blindsight and some develop nearly normal conscious vision, despite similar lesions to the occipital cortex. In the present study, we describe patient G.S., who has a unilateral congenital lesion of the optic radiations similar to the cohort of subjects we described in a previous study (Tinelli et al., 2013), except that the lesion was probably acquired during gestation. Unlike the previous report, patient G.S. shows *conscious* and strong residual vision in the contralesional hemifield. A combination of fMRI and DTI (Diffusion Tensor Imaging) results suggests that this *conscious* residual vision may be mediated by a massive reorganization of white matter tracts and visual cortical areas.

## 2. Patient and methods

### 2.1. Clinical description

G.S. was born at term in 2006. She was referred to Stella Maris Hospital at 6 years of age for reading problems, mainly a difficulty in shifting gaze to the next text line after a right-to-left saccade. For this reason, she underwent a complete neuropsychological assessment including a Wechsler Intelligence Scale for Children, which revealed an Intelligence Quotient (IQ) in the normal range. A complete ophthalmological evaluation revealed no refractive error or strabismus. Preliminary assessment of the visual field by means of manual kinetic Goldmann perimetry, showed a reduced sensitivity on the periphery of the left-hemifield (beyond 30° of eccentricity). The visual deficit was confirmed by an automated perimetry system (KOWA AP 340: similar to the Humphrey perimeter) in which luminance detection was tested for each eye for target locations spanning an area of 120 × 120°of visual field (see panel A of Fig. 2). No epileptic symptoms have been reported to date.

According to the medical history, at birth G.S. was diagnosed for an enlarged head circumference and in the subsequent two months an abnormal growth of the head was observed. At 3-months of age, ultrasound and MRI disclosed an atypical choroid plexus papilloma of the right lateral ventricle compressing the parieto-temporo-occipital cortex. Brain surgery removed the tumor, which resulted in a severe lesioning of the optic radiations connecting the visual thalamus with the right occipital cortex. At the bioptic exam the tumor was classified as a subependymal giant cell astrocytoma (Fig. 1). No specific neurological motor consequence was reported.

### 2.2. Psychophysical tests

All visual stimuli were generated by a Cambridge VSG 2/5 framestore and presented with a refresh rate of 100 Hz on a Pioneer color plasma monitor subtending 80° × 60° at a viewing distance of 57 cm. Stimuli were always presented on a mid-gray background and throughout the session, the subject was instructed to keep fixation on a central red disk subtending 0.2° with fixation visually monitored by an experimenter. All trials in which an eye movement was detected during the presentation of the stimuli were discarded from data analysis.

Contrast sensitivity for orientation discrimination was measured

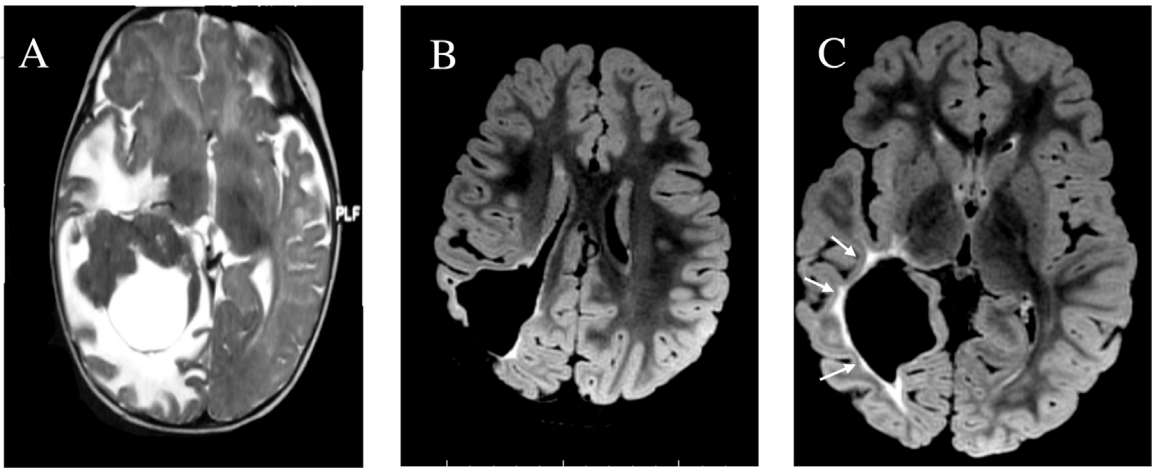


**Fig. 1. Pre and post surgery MRI scan**. Panel A: Pre-surgical MRI T2-weighted image on the axial plane. Intra-cerebral intra-ventricular edematous expansive lesion with wide compressive effect on deep temporo-parietal-occipital region and the surface of the brain. Panel B, C: Post-surgical MRI FLAIR-T2 images on the axial plane. Wide porencephalic post-surgical intra-axial cavity, communicating with lateral ventricle and brain surface (B). The hyperintensity relative to gliosis surrounding the post-chirurgical cavity follows the hypothetical stream of the optic radiations (C, white arrows).

with sinusoidal gratings (SF 0.5 cyc/deg) windowed in a square aperture of 8° presented for 200 ms on the monitor midline at a given horizontal eccentricity relative to fixation point (either 30° or 50°, tested in different sessions). The subject indicated whether the orientation of the stimulus was vertical or horizontal in a two-alternative forced choice (2AFC) paradigm. We calculated the proportion of trials in which the patient correctly reported the orientation of the stimulus as a function of contrast. The data (about 80 trials) were fitted with cumulative Gaussian curves and thresholds were calculated as the contrast level yielding 75% of correct responses.

To measure contrast sensitivity for stimulus detection, the grating was displayed at one of two horizontal eccentricities (30° or 50° tested in different sessions) with an elevation of ± 10° relative to the monitor midline. The patient's task was to report whether the stimulus was located above or below the midline. In both experiments, all stimuli were presented in the left hemianopic field of the patient G.S.

We measured the visual acuity of G.S. using a central grating of 1 cyc/deg vignetted in a squared window of 16° with a Michelson contrast equal to 90% and presented for 200 ms. In order to alter the perceived spatial frequency of the grating between 1 and 6 cyc/deg while keeping the eccentricity of the stimulus constant (≈ 26°), we varied the viewing distance (between 57 and 342 cm) and the eccentricity of the fixation point (between 28 and 164 cm). In trials where the distance of the grating from fixation had to be larger than the size of the monitor, the patient fixated on an illuminated spot located outside the screen. In a 2AFC task, the patient indicated the orientation of the grating (vertical or horizontal). Similar tests were performed in one normal subject of matched age.

## 2.3. fMRI

### 2.3.1. Data acquisition

fMRI scanning was performed when the girl was 7 years old with a GE 3T scanner (Excite HDx, GE Medical Systems, Milwaukee, WI) at the Fondazione CNR/Regione Toscana G. Monasterio in Pisa, Italy. The study was approved by the ethics committee of the Azienda Ospedaliera-Universitaria Pisana (protocol number 3255, approved on 20/01/2009) and was in accordance with the ethical standards of the 1964 Declaration of Helsinki. Informed written consent was obtained from the patient's parents prior to the scanning session, in accordance with the guidelines of the MRI Laboratory. The fMRI session consisted of four functional and one structural scans. Three-dimensional (3-D) anatomical images were acquired at 1 × 1 × 1 mm resolution using a T1-weighted magnetization-prepared fast Spoiled Gradient Echo (SPGR) sequence (FOV = 256 mm, BW = 15.63, 256 × 256 matrix, TE = minimum full). For the acquisition of retinotopic maps Echo Planar Imaging (EPI) sequence was used (FOV = 240 mm, 128 × 128 matrix, slice thickness = 4 mm, 30 axial slices, flip angle = 90, TE = 40 ms, TR = 2500 ms). The first 13 s of each functional acquisition were discarded from data analysis to achieve a steady state.

### 2.3.2. Anesthesia

Intravenous pharmacologically-induced sedation was used when performing morphological and functional MRI. The induction was performed in spontaneous breathing using a mixture of air, oxygen and 6% Sevorane; vital parameters (SaO2, HR, BP and ET CO2 by nasal cannula) were monitored. Anesthesia was maintained using an infusion of Propofol 1% 8 mg/kg/h after positioning a 22 g vein catheter. Spontaneous breathing was maintained during sedation adding 4lt/min oxygen through a nasal cannula. The left eye was kept open using a medical adhesive tape and was protected by applying ophthalmic gel (Carbomer 974P) every 40 min. The pharmacological sedation was sufficient to stop eye movements. Gaze direction was measured before and after the BOLD scans and the value resulted to be equal in 1° precision.

### 2.3.3. High luminance flicker stimulus

During fMRI scanning, 15 s of full-field flashing stimuli (100 cd/m$^2$ at 0.5 Hz: 1000 ms on and 1000 ms off) alternated with 15 s of blank period, repeated six times. Stimuli were delivered through a custom-made optic fiber bundle designed by our group (Greco et al., 2016).

### 2.3.4. pRF mapping stimuli

Stimuli were projected on a wide visual field ( ± 40°) through a custom-made magnetic-imaging-compatible visual projection system designed by our group (Greco et al., 2016). Spatial resolution was 10,000 pixels corresponding to the number of optic fibers in the projection system and temporal resolution was 60 Hz.

Population receptive field maps were constructed using (i) horizontal and vertical meridian stimulation, (ii) upper, lower, left and right stimulation of the four visual quadrants, and (iii) upper, lower, left and right *peripheral* stimulation of the four visual quadrants. Stimuli were generated using routines from the Psychtoolbox (Brainard, 1997; Kleiner et al., 2007) controlled with MATLAB programs (The

MathWorks, Natick, MA).

For (i) we used stimuli comprising 100 circular dots, half black and half white, moving on a grey background in two symmetrical sectors across the fixation point along the two principal meridians (Engel et al., 1997; Sereno et al., 1995; Wandell et al., 2005). Each dot had a lifetime of 20 frames or 333 ms at a refresh rate of 60 Hz (local speed at linear trajectory = 6.5 degs$^{-1}$). A block design was used with meridians stimulated interchangeably (6 repetitions) for 15 s and motion direction inverting seven times to avoid BOLD adaptation. For (ii) we used stimuli comprising 250 circular dots, half black and half white, moving on a grey background in four quadrants. A block design was used with quadrants stimulated sequentially clockwise, starting from the upper right. All other information is identical to (i). For (iii) we used the same stimuli as in (ii) with the only difference that stimulation was limited to beyond 20° of eccentricity.

#### 2.3.5. Data analysis

Data were analyzed by BrainVoyager QX (Version 20.2, Brain Innovation, Maastricht, Netherlands) and MATLAB (MathWorks, MA). Prior to statistical analysis, functional data underwent pre-processing steps including 3-D motion correction, linear trend removal and high pass filtering. Slice scan time correction was performed for functional data.

Functional data were co-registered on the 3D anatomical T1-weighted images by using a gradient-based affine alignment with the standard BrainVoyager nine parameters (three for translation, three for rotation and three for FOV scale).

#### 2.3.6. Evaluation of fMRI activity

BOLD responses were analyzed using a General Linear Model (GLM) by convolving a box-car function for each stimulation block with a canonical hemodynamic response function (HRF). For each region of interest (ROIs), average BOLD percentage signal change was calculated.

#### 2.3.7. Estimation of pRF maps

We use in-built BrainVoyager QX (v.20.2) routines for pRF estimation which uses the two-dimensional Gaussian pRF model (Dumoulin and Wandell, 2008):

$$g(x, y) = e^{-\left(\frac{(x-x_0)^2+(y-y_0)^2}{2\sigma^2}\right)}$$

where $x$ and $y$ define the centre of the pRF in the visual field and $\sigma$ the radius. The visual field is defined as 40° on either side of the centre of the visual field in the horizontal (x) dimension and 28° on either side along the vertical (y) dimension. The range of pRF sizes is 0.2–7°, in 30 equal steps. Subsequently, the visual field is divided into a 30 by 30 grid. For each TR, we use the corresponding binarized stimulus frame (stimulated area is white; background is black) irrespective of stimulus carrier and created a binarized version stimulus movie. The number of frames in the movie corresponds to the total number of volumes used, equal to 360. A positive response is predicted whenever a stimulus falls on a pRF and the prediction is convolved with the hemodynamic response function (HRF). The best model fit for each voxel is obtained by finding values that maximized the correlation between the predicted and actual BOLD response.

### 2.4. DTI

#### 2.4.1. Data acquisition

DTI data was acquired with 30 diffusion directions and 5 non-weighted images with the following parameters: B0 = 1000 s/mm$^2$, TR = 16,000 ms, TE = 85.4 ms 57 slices, in plane resolution = 2 mm and slice thickness = 2.4 mm.

#### 2.4.2. Software

Anatomical and diffusion data was analyzed with FMRIB Software Library v 5.0 FMRIB software library (http://www.fmrib.ox.ac.uk/fsl/fdt/index.html) (Jenkinson et al., 2012).

#### 2.4.3. Pre-processing

B0 images were pre-processed using the BET tool, which resulted in the segmentation of the brain from the skull tissue. The derived mask was used to separate the non-diffusion from the diffusion space. Eddy current correction was performed and the results were applied accordingly to the b-vectors. Diffusion parameters were fitted using DTIFIT to obtain fractional anisotropy (FA), mean diffusivity (MD) and radial diffusivity (RD) maps and a probabilistic diffusion model was estimated with BEDPOSTX. The FA map was used to register the diffusion data to the anatomical space using FLIRT's affine registration. The resulting matrix was inverted to allow transformation of volume-of-interests (VOIs) to the DTI native space. VOIs used as seeds for tracking were functionally defined using fMRI and pRF results in BrainVoyager QX v.20.2. Subsequently, these were first transformed into NIfTI file format using BrainVoyager's NIfTI Converter plug-in (v.1.09) and then further transformed into DTI native space using the inverted matrix from the affine registration.

#### 2.4.4. Tracking

Estimation of tracts was performed using *probtrackx2* (Behrens et al., 2003; Johansen-Berg et al., 2004) initializing 5000 streamlines from each voxel in the seed mask with the step size of 0.5 mm and curvature threshold of 0.2. Fiber tracking was performed in the native diffusion space between the subsequent ROIs; the lateral geniculate nucleus (LGN), V1, and MT+. The ROIs were first defined by experienced child neuro-radiologist, then we verified that the ROI had a significant BOLD response to the flashing stimuli both for the lesioned and normal hemifields. In addition we also checked that the ROI positions were consistent with the Juelich atlas (Malikovic et al., 2007).

For each pair of regions, tracking was performed twice using each region once as a seed and once as a target. All voxels in each of the resulting maps consisted of the number of streamlines, which were not rejected during the tracking process. The accepted streamlines for the two directions were summed for each anatomical position, allowing the estimation of the trajectory of the most probable tracts connecting the two ROIs. The tracts are illustrated in a heat color map scaled to the maximum streamline of the labeled voxels. Obtained tracts were thresholded by the value equal to the 40% of the 95 percentile of the distribution of the intensity values in the tract (Galantucci et al., 2011). To obtain mean FA, MD and RD, thresholded tracts were binarized and then multiplied by each of the DTI scalar maps values (FA, MD, RD). Similarly to Ajina et al. (2015a) we resampled the tracts bilaterally for patient G.S. and a healthy control to 100 nodes, distributed equally along the length of the tract (Yeatman et al., 2012). The region between nodes 15 and 85 was then used to represent 'whole tract' profiles, with the proximal and distal 15 nodes ignored to remove potential contamination with grey matter voxels or partial volume effects.

## 3. Results

### 3.1. Psychophysics

We assessed the visual field of patient G.S. by means of an automated perimetry system (KOWA AP 340: similar to the Humphrey perimeter). Each eye was tested on 79 different locations (to cover a field of view of 120 × 120°) with light targets of varied luminance

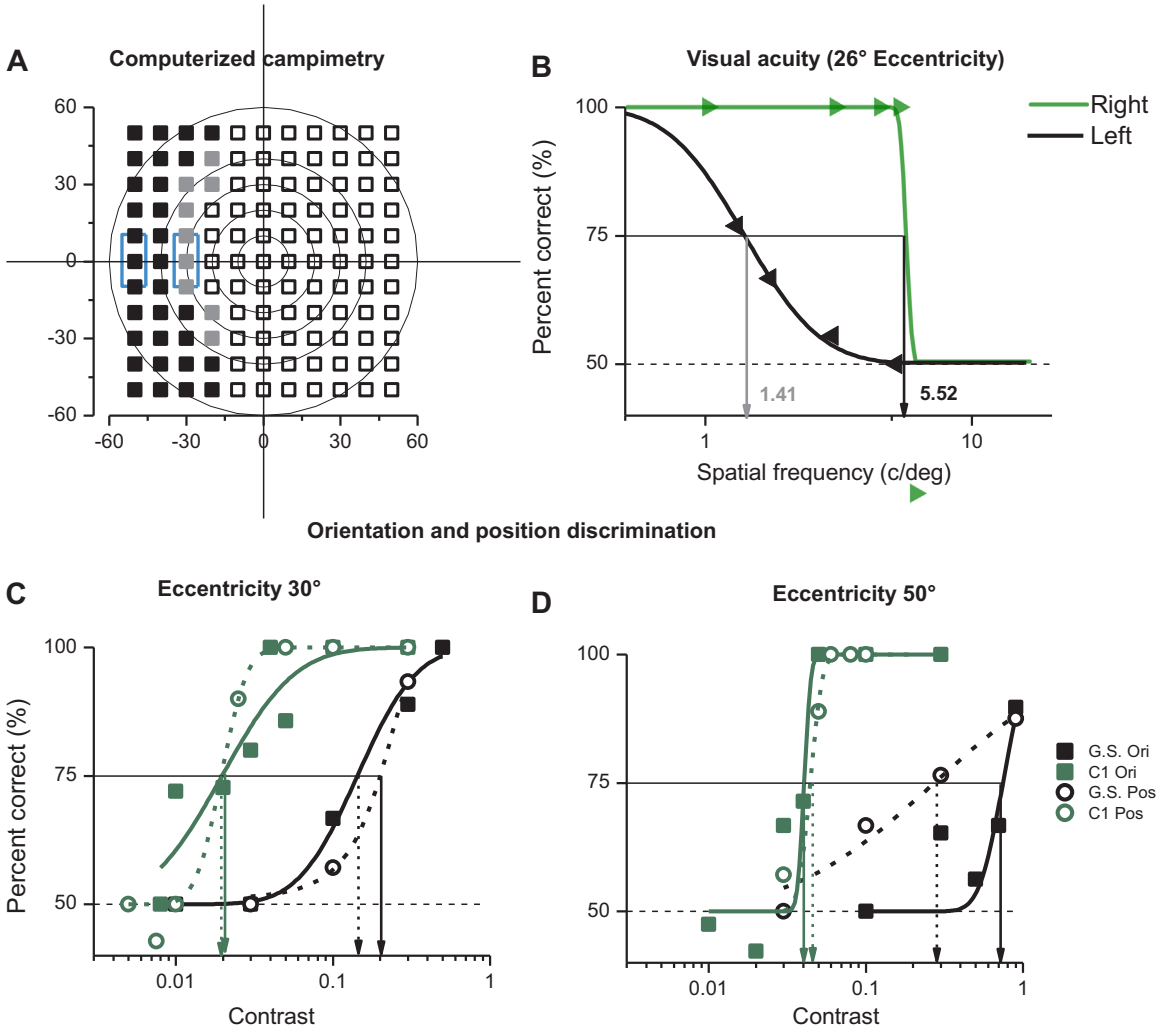


**Fig. 2. Psychophysical assessment of visual performance in patient G.S. and an age-matched control (C1)**. Panel A: Visual field perimetry obtained with the KOWA re-sampled at 10° resolution. Solid black squares indicate test points in which targets were missed even at maximum luminance intensity. Section of the visual field in which stimulus detection was partially compromised (e.g. target detection accomplished with intermediate luminance levels) are indicated by gray squares whilst white open symbols indicate areas of the visual field in which detection performance was optimal. Light blue boxes on the left side indicate the stimulus position ranges stimuli for the orientation and position discrimination task (C/D). The width of the boxes represent stimulus size, the centre of the boxes indicates the tested eccentricity (30° or 50°) whilst box height represent the maximum vertical jitter of the stimulus positions. Panel B: Visual acuity of patient G.S. at 26° horizontal eccentricity as derived from an orientation discrimination task. Data for the spared and lesioned hemifields are shown in different colors (green and black respectively). While acuity in the right visual field was found to be close to that of age-matched controls (see text for details), on the left visual field acuity was strongly reduced, by about a factor of 3 (threshold at 75% of correct responses equal to 1.41 cyc/deg). Panel C-D show contrast sensitivity for two different tasks, position and orientation discrimination at 30° and 50° of horizontal eccentricity. For both eccentricities, sensitivity for position discrimination for patient G.S was found to be around 1 log unit lower than the age-matched control (open circles). A similar difference did hold for orientation discrimination at 30° (green and black squares in C) but not at 50° of eccentricity where the impairment is about 3 times stronger (green and black squares in D). (For interpretation of the references to color in this figure legend, the reader is referred to the web version of this article.)

while fixation was monitored throughout the session. As shown in Fig. 2A, patient G.S. was able to detect all the targets presented in the right hemifield. G.S. also detected all the targets presented within the first 25° of the left hemifield but showed reduced sensitivity for stimuli presented around 30° (grey area in Fig. 2A). The patient was unable to detect most of the targets located at more extreme eccentricities.

According to the perimetry, deterioration of visual abilities in the left hemifield of subject G.S. starts around 25° of eccentricity. To assess the residual visual abilities in the hemianopic hemifield, we performed a 2AFC discrimination threshold for contrast and acuity. G.S. was always conscious of the display of transient supra-threshold stimuli and reported their presence with great confidence. Spatial acuity on the spared (right) hemifield was close to that of age-matched controls (≈ 5 cyc/deg) as derived from Battista et al. (2005). Visual acuity at 26° eccentricity in the left hemifield is about 1.6 cyc/deg (Fig. 2B). Although the value is about three times lower than the normal acuity, it is sufficient to mediate good vision.

G.S. also had normal ability to consciously detect low spatial frequency gratings at high contrast (4° radius, spatial frequency 0.5 cyc/deg, luminance contrast 40%). G.S. showed 100% detection performance in all parts of the visual field, including the peripheral visual field (30° and 50°) in which light detection of small stimuli was either compromised or abolished according to the perimeter data. To investigate this further, we measured contrast thresholds with two different tasks (localization and orientation discrimination – see Section 2 for details) at two eccentricities: 30° and 50°. At 30° G.S. had similar contrast thresholds for orientation discrimination and stimulus localization around 15–20% of Michelson contrast (data in black in Fig. 2C), an impairment of about one log unit compared to an age-matched control (threshold around 2% - green data in Fig. 2C). By increasing the eccentricity from 30° to 50° (Fig. 2D), contrast thresholds for position discrimination in patient G.S. increased by a factor of ≈ 2 (from 15% to

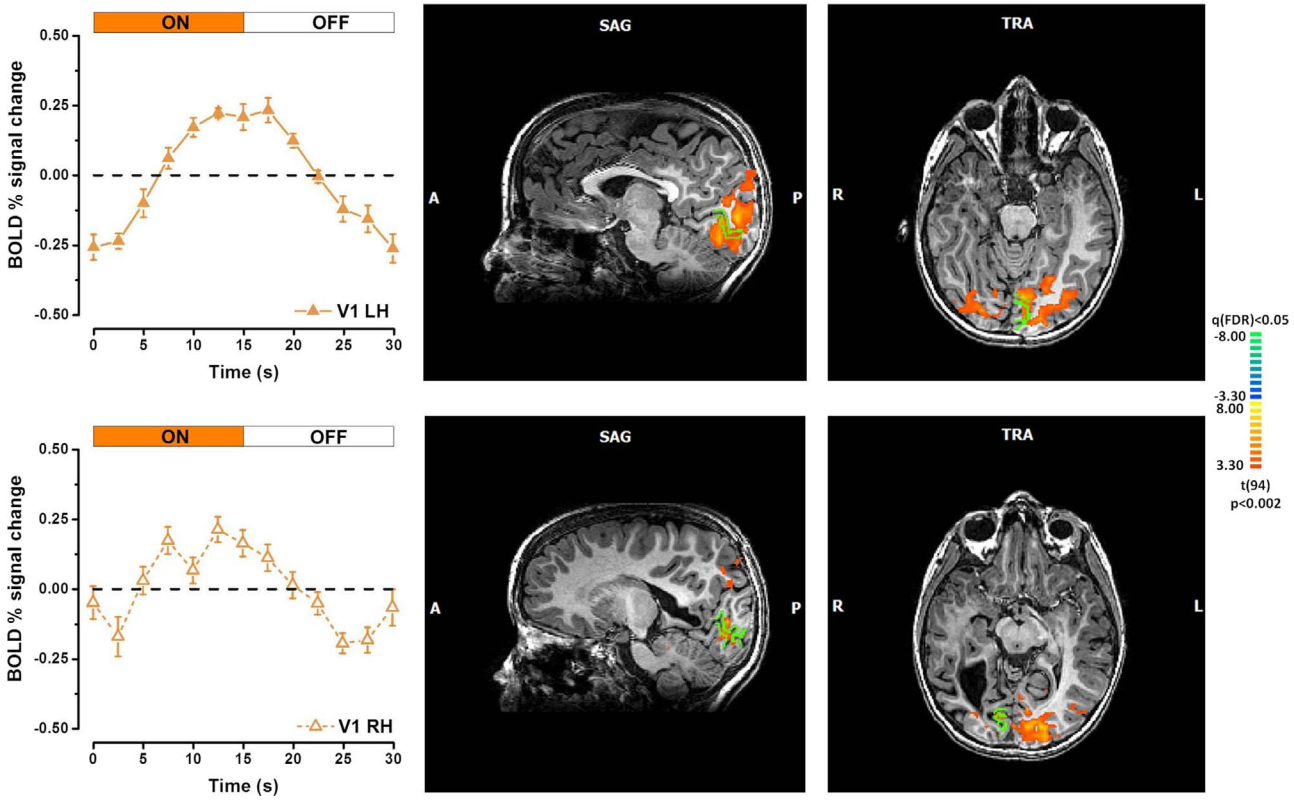


**Fig. 3.** BOLD responses in the left and right V1 (top and bottom row respectively) to the flicker stimulus overlaid on anatomy in native space. The calcarine sulci, where V1 is located, are labeled in green. The graphs show average percentage signal change over 30 s (15 s on; 15 s off) averaged over six repetitions in left and right V1. (For interpretation of the references to color in this figure legend, the reader is referred to the web version of this article.)

30% of contrast- black dashed vertical arrows in Fig. 2C–D), an amount similar to that observed in the control subject (from 2% to 4% - green dashed vertical arrows in Fig. 2C–D). However, orientation discrimination at 50° was severely impaired in G.S. with contrast thresholds around 80%, 20 times higher than the threshold of the age-matched control (compare green and black solid vertical lines in Fig. 2D). These data show that although localization of large stimuli is still possible inside the dense scotoma, orientation discrimination is heavily impaired, suggesting abnormal visual processing in this part of the visual field.

### 3.2. Cortical BOLD responses

We measured BOLD responses to a spatially homogenous high-luminance flicker to explore stimulus-induced activity in the visual cortex of patient G.S. Figs. 3 and 4 show BOLD activity overlaid on anatomy in native space. The right hemisphere of G.S. has a large temporo-parieto-occipital lesion with some sparing at the occipital pole (Fig. 3). V1 in the intact hemisphere shows strong BOLD responses to our flicker stimulus, whereas activity in the lesioned V1 is limited to a more anterior position along the calcarine sulcus. BOLD activity in extrastriate areas of the lesioned hemisphere (possibly V2 and V3) is reduced compared to activity in the very same cortical areas in the intact hemisphere. In both hemispheres, some BOLD activity extends within the parieto-occipital sulcus.

Fig. 4 shows BOLD activity in response to flicker stimulation in a position that in healthy controls corresponds to MT+ in the left hemisphere (first row). Interestingly, activation is also present in a corresponding region in the lesioned hemisphere as assessed by an experienced neuroradiologist. The BOLD response is statistically significant, albeit comparatively reduced in the lesioned hemisphere.

### 3.3. Population receptive field mapping

Subsequently we used a powerful model-driven approach – population receptive field (pRF) mapping – to investigate whether cortical areas, found to respond to the high-luminance flicker stimulus, maintain a retinotopic organization. The method pools together all stimulus sequences (a total of 360 TRs/volumes) and verifies whether the response is consistent with a retinotopically-organized spatial map. Fig. 5 shows thresholded (r > 20%) eccentricity maps along the horizontal dimension. In the absence of any cortical damage, stimuli positioned in the left hemifield are processed in the right visual cortex and vice versa. In patient G.S., the left primary visual cortex maintains a normal representation of the right visual field, with central vision processed posteriorly near the occipital pole and more peripheral eccentricities processed anteriorly along the calcarine sulcus (Fig. 5b, f). In the primary visual cortex of the lesioned hemisphere, we observed no such retinotopic organization. It appears that the cortical area in the right V1 responding to the high-luminance flicker does not show any consistent retinotopic mapping. This result is surprising if we take into account that the residual visual abilities of patient G.S are quite good within the central 30° of the visual field contralateral to the lesioned hemisphere, as shown by the psychophysical tests.

The MT+ complex in the intact hemisphere contained a representation of both the contralateral (Fig. 5b – white arrow) and ipsilateral visual fields (Fig. 5a, c – striped arrows). Although ipsilateral activity in MT+ has been previously reported (Huk et al., 2002), in patient G.S. this activity is more prominent than the contralateral one and extends up to 35 degrees of eccentricity. In the MT+ complex of the lesioned hemisphere, we observed an island of contralateral representation up to ≈ 15 degrees of eccentricity (Fig. 5c – white arrow). In an adjacent and more posterior area, which could potentially correspond to LOC, we report ipsilateral visual field representations (Fig. 5d - striped arrow). All these data suggest a retinotopic re-

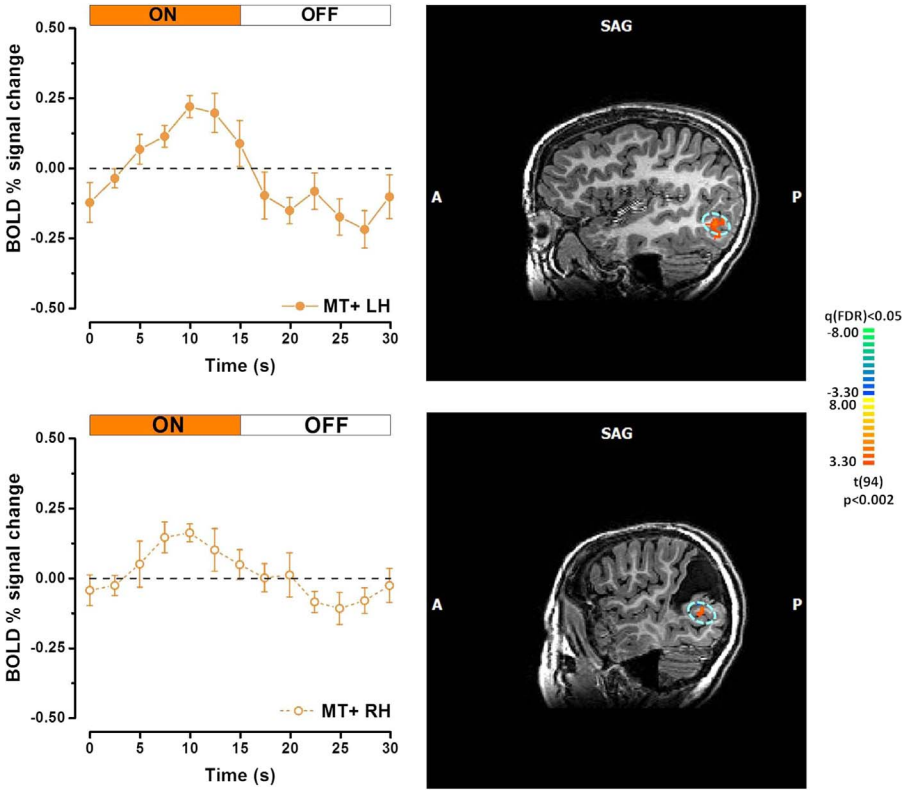


**Fig. 4.** Cortical BOLD activity in the left and putative right MT+ (top and bottom row respectively) in response to the flicker stimulus overlaid on anatomy in native space. Light blue ovals indicate the MT+ clusters. The graphs show average percentage signal change over 30 s (15 s on; 15 s off) over six repetitions. (For interpretation of the references to color in this figure legend, the reader is referred to the web version of this article.)

organization at various extrastriate cortical areas in both hemispheres.

We also observed intermingled islands of contralateral and ipsilateral visual field representation along the parieto-occipital sulcus (POS) of the intact hemisphere (Fig. 5e, f), at cortical locations responsive to the high-luminance flicker stimulus. Considering that no retinotopic organization was observed in the primary visual cortex of the lesioned hemisphere, it is likely that the MT+ complex together with the POS in the intact hemisphere may sub-serve the residual visual abilities of patient G.S., at least for the residual vision of far eccentricities (> 20 deg) that are not represented in the lesioned hemisphere.

### 3.4. Probabilistic tracking

Next, we used DTI to explore the structural connections subserving visual functions in patient G.S. The LGNs, V1 and MT+ ROI were defined anatomically with the help of an experienced neuroradiologist and on the response to high-luminance flicker stimuli and pRF results (see Table 1 for the number of voxels in each ROI details). The size of the calcarine sulcus in the right (lesioned) hemisphere was reduced compared to the left (intact side) due to the location of the lesion. This resulted in a smaller right hemisphere V1 ROI used for tractography.

Fig. 6 shows the white matter tract running between LGN and V1 in the left and right hemispheres. The geniculo-striate pathway is preserved in the intact hemisphere, but as expected by the anatomical location of the lesion it is severely compromised in the right hemisphere: only 0.09 streamlines on average were accepted for the lesioned hemisphere against 97 for the intact hemisphere (see Table 2).

After a threshold set to accept the 40% of the 95% confidence limit of the number of streamlines (Galantucci et al., 2011), the tract appears broader than in the normal hemisphere, consistent with a decrease of FA for the lesioned hemisphere. Interestingly, this minor tract reached calcarine sulcus through two branches encompassing the lesion as shown in Fig. 6.

The opposite pattern of results is observed for the LGN-MT+ tract (Fig. 7), where we measured an enhanced connectivity between LGN and MT+ in the lesioned compared to the intact hemisphere (38.6 streamlines of the lesioned versus 3.57 for the intact hemisphere). This result is consistent with the evident retinotopic organization observed in the lesioned MT+ complex using the pRF approach, but not in V1 of the same hemisphere. A similar pattern of results was obtained when we repeated the analysis with a bigger ROI in the intact hemisphere, reinforcing the result of a stronger anatomical connection between the visual thalamus and MT+ in the lesioned respect to the intact hemisphere.

## 4. Discussion

Despite a massive lesion in the right hemisphere resulting in a nearly complete lesion of optic radiations and a disconnection of V1 from LGN, patient G.S. shows a surprisingly good residual vision. Neither the parents nor the teachers or the doctors realized that the child had reduced visual sensitivity in the left peripheral hemifield before the age of 7, when the patient was referred to the Stella Maris Hospital for a suspected reading disability. The computerized perimetry indicated that light detection in the left hemifield was almost completely preserved up to 25° along the horizontal axis. At more extreme eccentricities target detection was compromised with a slightly better performance in the upper visual field.

The reduced visual acuity of about a factor of 3 at an eccentricity of 26° (1.4 cyc/deg versus 5.5 cyc/deg) complements the visual perimetry data and indicates that, at peripheral locations in which light detection was compromised, the ability to parse stimulus details was strongly reduced, suggesting a distortion of visual spatial maps. Such a distortion is also consistent with the observed difference between contrast thresholds for position and orientation discrimination. The data indicate that the cortical reorganization in patient G.S. was able to mediate rudimental contrast analysis to serve stimulus localization, but not a more sophisticated analysis required for acuity or orientation discrimination.

What brain circuitry mediates vision in the hemianopic hemisphere

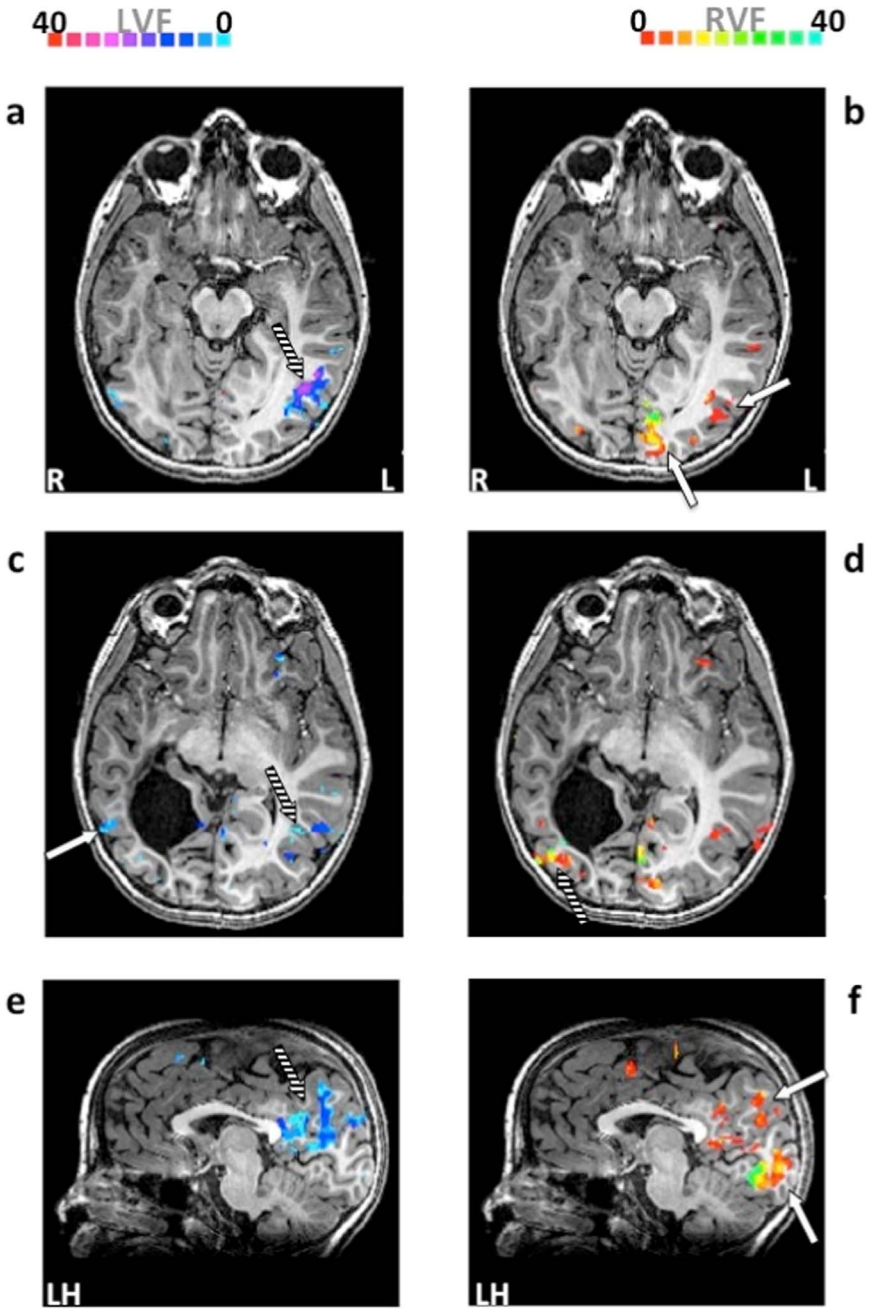


**Fig. 5.** Eccentricity maps along the horizontal dimension generated using the pRF approach, in patient G.S. White and striped arrows indicate contralateral and ipsilateral visual field representations respectively. The primary visual cortex of the intact hemisphere has a normal eccentricity representation of the contralateral visual field (b, f). No retinotopic organization is evident in the primary visual cortex of the lesioned hemisphere. The left MT+ complex contains representations of both contra- and ipsilateral visual fields, with an over-representation of the latter up to 30 degrees of eccentricity (a, b, c). Similarly, the right MT+ complex has representations of only the contralateral visual fields for eccentricity less than 15 degrees (white arrow- c). Intermingled islands of contralateral and ipsilateral visual field representations can be seen along the POS of the intact hemisphere (e, f).

**Table 1**
Number of voxels in DTI space for each ROI. The number of accepted streamlines was normalized each time to account for the number of voxels in the DTI seed.

| | Number of voxels in DTI space | |
|---|---|---|
| | **RH** | **LH** |
| **LGN** | 61 | 59 |
| **V1** | 592 | 835 |
| **MT+** | 478 | 283 |

of G.S.? Probably not V1 of the lesioned hemisphere, as the lesioned calcarine region receives little input from the LGN and does not show any retinotopic organization but only a general response to high-luminance flicker. BOLD activity in the intact (left) V1 is normal and cannot account for the residual vision in the ipsilateral hemifield. The population receptive field mapping showed that the left V1hasa normal retinotopic representation of the contralateral visual field and it does not respond to stimuli presented in the ipsilateral visual field. We observed islands of representation of the hemianopic visual field in MT+ of the lesioned (right) hemisphere. This contralateral representation was found to be limited to the first ≈ 25° of the left visual field. G.S. has a near-to-normal vision for this part of peripheral field, reinforcing the suggestion that the right MT+ plays a role for this surprisingly good vision.

The intact (left) MT+ complex also shows a representation of the ipsilateral visual field, which is paradoxically more pronounced than the contralateral representation. It is also more extensive compared with healthy controls (Huk et al., 2002). Similarly to MT+, the POS in the intact hemisphere of G.S. maintains intermingled islands of contralateral and ipsilateral visual field representations. This result is surprising, considering that in healthy adults, cortical areas in the POS, such as V6 and area prostriata only have contralateral visual field representations (Mikellidou et al., 2017; Pitzalis et al., 2010). These

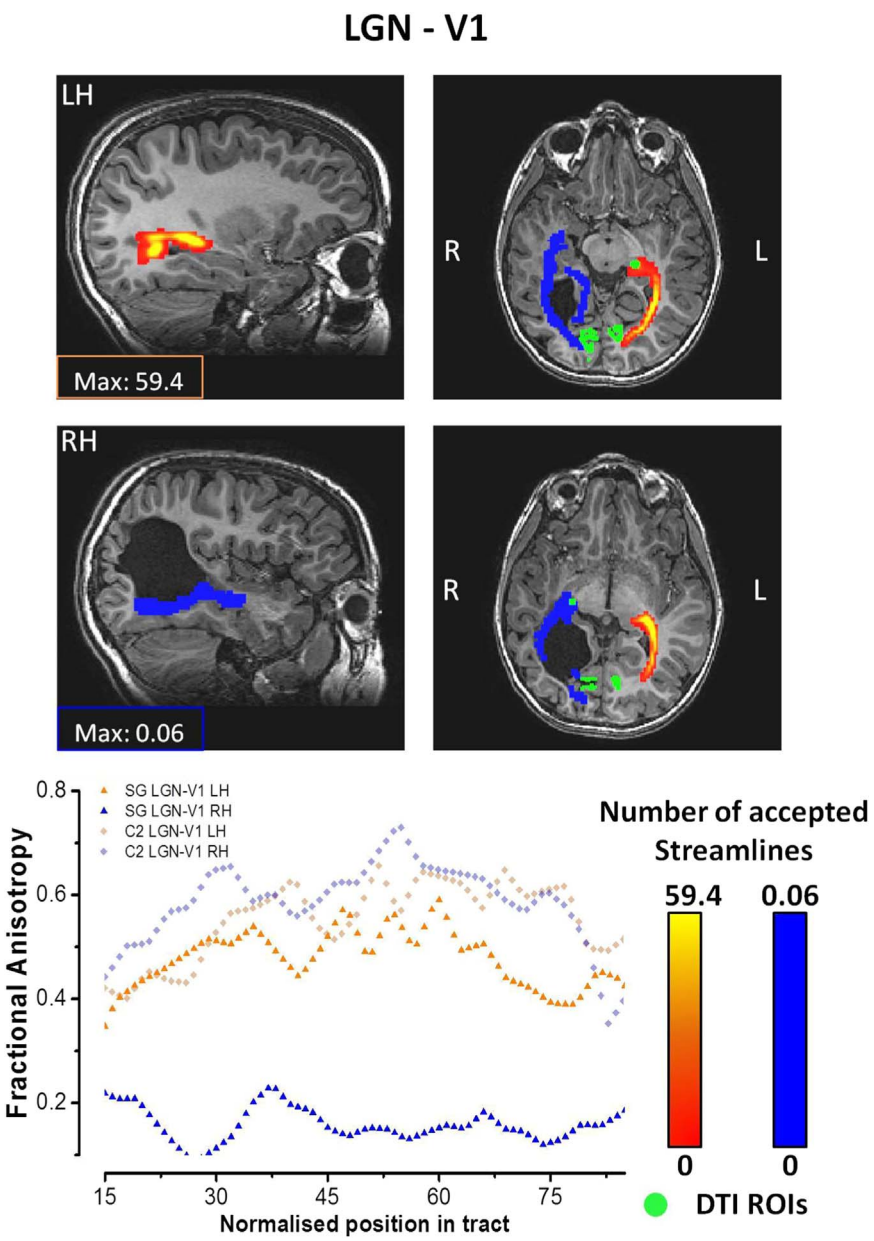


**Fig. 6.** White matter tracking between LGN-V1 performed independently in the two hemispheres. Whilst the LGN-V1 tract in the intact hemisphere appears normal both in terms of accepted streamlines and FA, the same tract in the lesioned hemisphere is severely compromised. For each tract, probabilistic tracking was performed twice between two regions-of-interest, with each ROI acting once as a seed and once as a target. The number of accepted streamlines was first determined for one direction (i.e. LGN-V1), then normalized for the number of voxels in the seed (LGN) and finally threshold at the 40% of the 95th percentile, similar to Galantucci et al. (2011). The same process is repeated for V1-LGN and the two tracts are added voxel by voxel to generate the map in figures. The normalized FA along the two tracts shows that the intact hemisphere of G.S. is similar to a healthy control.

**Table 2**
DTI scalars: mean values and standard deviation for fractional anisotropy (FA), mean diffusivity (MD), radial diffusivity (RD) and accepted number of streamlines for LGN-V1 and LGN-MT+ tracts in each hemisphere.

| | Tract | Mean FA | Mean MD $*10^{-4}$ | Mean RD $*10^{-4}$ | Streamlines |
|---|---|---|---|---|---|
| LH | LGN - V1 | 0.47 (0.13) | 8.7 (1.6) | 1.0 (1.8) | 97.0 |
| | LGN - MT+ | 0.42 (0.08) | 8.3 (0.7) | 9.9 (0.8) | 3.57 |
| RH | LGN - V1 | 0.18 (0.10) | 14.6 (5.1) | 15.7 (5.1) | 0.09 |
| | LGN - MT+ | 0.15 (0.06) | 17.3 (4.7) | 18.4 (4.6) | 38.6 |

ipsilateral representations cover the first 35 degrees of the visual field and may well sub-serve the residual vision for these eccentricities. If so, the ipsilateral cortical involvement of these high associative areas could explain the discrepancy in performance between the orientation and the position discrimination tasks.

These considerations are also in agreement with the tractography results. The thalamic- MT+ tract is relatively stronger for the lesioned than the intact hemisphere. In non-human primates this tract is prominent at birth and is heavily pruned during development to practically disappear in adulthood (Bourne and Morrone, 2017; Cowey et al., 1994; Nakagawa and Tanaka, 1984; Warner et al., 2010, 2012). The time of pruning coincides with the maturation of the feed-forward connection from V1 to MT+. In human infants the V1-MT+ connectivity is still not mature at 8 weeks of age, while MT+ shows already a good selectivity for motion at the same age (Biagi et al., 2015). This suggests that the thalamic-MT+ projections may be stronger also in humans, as it occurs in marmosets. Interestingly, patients with blindsight usually have more pronounced connections between the LGN and MT+ compared with patients without blindsight despite similar brain lesions (Ajina et al., 2015b; Tamietto and Morrone, 2016). Patient G.S., who probably acquired some initial lesion of the optic radiations at an embryonic stage due to the compressive effect of the tumor, seems to have preserved this strong connection between LGN and MT+ in the lesioned side, consistent with a decreased innervation of MT+ from V1 later in life due to the lesion. In this light, we have to assume that MT+ in the lesioned

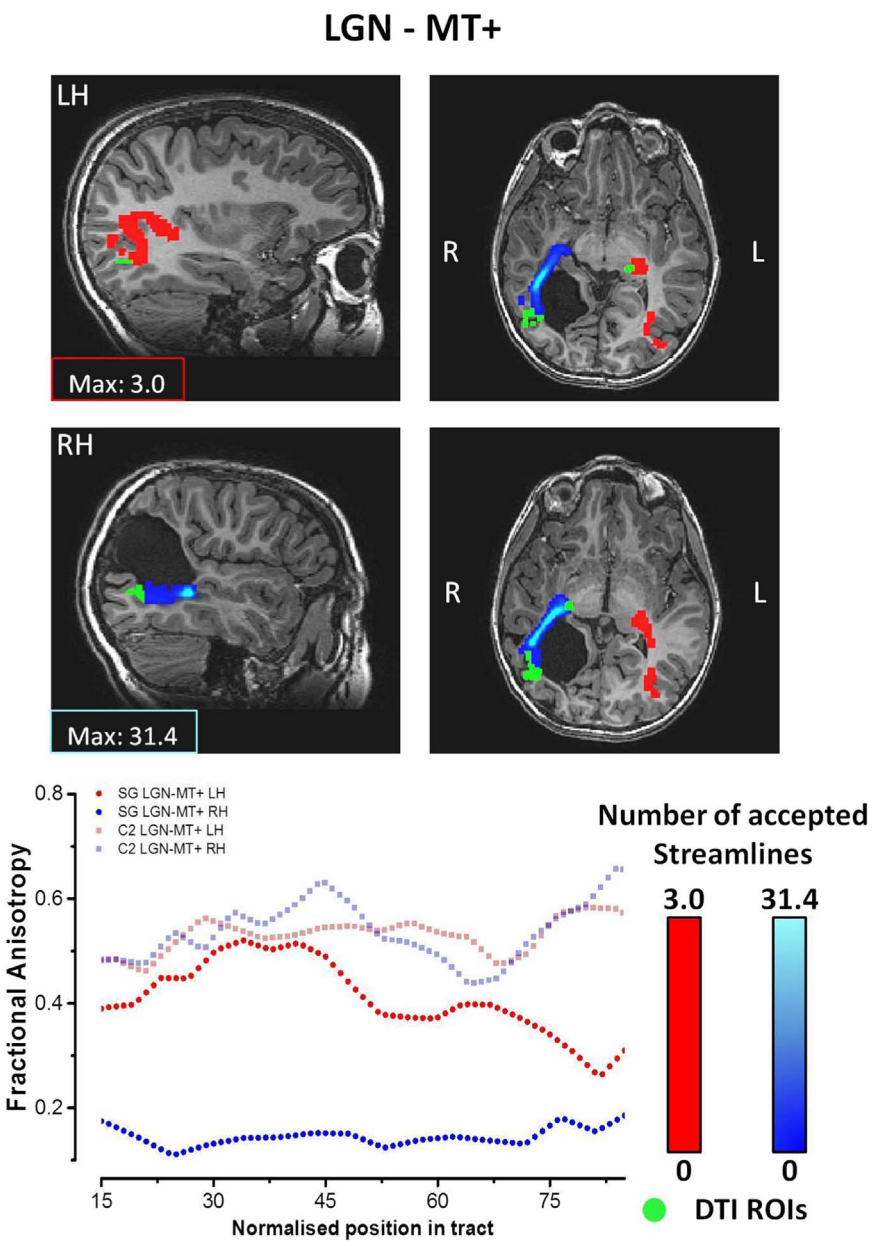


**Fig. 7.** White matter tracts between LGN-MT+. Similarly to the LGN-V1tract, we performed an independent analysis for the two hemispheres by running probabilistic tracking twice, with each ROI acting once as a seed and once as a target. The LGN-MT+ tract in the lesioned hemisphere is more prominent than in the intact hemisphere, although the FA along the tract shows that the integrity of white matter in the lesioned hemisphere is compromised compared to the intact side and a healthy control.

G.S. hemisphere is partially performing many of the functions usually mediated by V1.

It is interesting to compare patient G.S. with the four blindsight patients described by Tinelli et al. (2013), who had acquired similar brain lesions perinataly, resulting in the destruction of the optic radiations. The lesion in G.S. is less pronounced, allowing for the preservation of some associative cortex. This may have allowed the conscious vision for the central part of the controlateral visual field. Both G.S. and Tinelli et al.'s patients have ipsilateral representations of the visual field. In the two patients of Tinelli et al. tested with fMRI, an ipsilateral representation is also present in the intact calcarine sulcus, in addition to the POS. However, in patient G.S. the ipsilateral representation is mainly located in the temporal-occipital or POS regions. The perception of these patients is very different: whilst no residual conscious vision was reported for Tinelli et al.'s patients, G.S. has near-to-normal conscious central vision. The comparison between these patients leads to interesting suggestions. In all these patients there has been a strong cortical reorganization, probably involving subcortical re-routing of thalamic pathways. However, it seems more beneficial to vision to have a lesion that allows re-routing to the associative cortex of the same lesioned hemisphere as it is in G.S. This inevitably determines the amount and location of the ipsi- and contralateral cortical representation of space. The outcome of the residual vision may depend on this. It would be very interesting to determine the exact circuitry mediating good and conscious vision in G.S., but not in Tinelli et al.'s patients. It would also be important to verify whether MT+ of a lesioned hemisphere can really absolve the role of V1 and if this is a specific property of MT+ or can be extended to all extrastriate cortices (see Tamietto and Morrone, 2016). Another study suggests that this may be the case: in hemianopic adult patients with a lesion to V1, the positive correlation between MT+ activity and motion coherence of the stimuli is lost. Instead, MT+ showed a decreased BOLD response to motion coherence that resembles V1 response in healthy adults (Ajina et al., 2015a). Callosal connections between the two hemispheres could also help preserve some of the residual visual abilities of patient G.S.

Similarly, a loss of motion direction selectivity has been observed in the marmoset monkey with lesions acquired during the first weeks of life (Yu et al., 2013), reinforcing our interpretation of the data in G.S. However, at present further evidence is necessary before we can fully understand the minimal conditions to retain *conscious* vision despite a

massive V1 lesion.

Despite the challenges to uncover the mechanisms mediating awareness (for commentary see Berlucchi et al., 2017), it has been proposed that a fronto-parietal network plays a key role in the processes (Sanchez-Lopez et al., 2017; Passingham and Lau, 2017). Interestingly, this fronto-parietal network is also important for visuospatial attention which can modulate decision criteria and consequently awareness (Vernet et al., 2017). However, low-level cortical areas have also been assigned a fundamental role in visual awareness in line with reports of lesions to the primary visual cortex (V1) abolishing most conscious visual processing (Zeki, 1993). Two theories have been proposed to interpret the role of V1 lesions in visual awareness (Tong, 2003): hierarchical models suggest that *conscious* perception is mediated by higher-level extrastriate areas and V1 lesions interrupt their afference and the flow of incoming information (Crick and Koch, 1995; Rees et al., 2002). Interactive *models* suggest an active role of V1 in visual awareness through recurrent circuits (Bullier, 2001; Lamme and Roelfsema, 2000). This theory postulates that consciousness arises from the reverberating activity of feed-forward and feed-back loops between higher order visual cortices and V1. Given the existence of evidence in support of both theories, the role of V1 in visual awareness is still widely debated.

Unconscious vision can also be elicited in normal individuals in the laboratory. Binocular rivalry is one technique (Alais and Blake, 2005; Levelt, 1965; Lunghi et al., 2010); the other is interference with TMS. The perception of briefly presented static stimuli can be disrupted by applying transcranial magnetic stimulation (TMS) on the primary visual cortex (Corthout et al., 1999) around 100 ms after stimulus offset. The interference exerted after the stimulus onset can act by disrupting feedback signals from the extrastriate areas to V1, a result supporting the *Interactive models* idea based on recurrent circuits. On the contrary, a recent study by Mazzi et al. (2014) shows that two patients with unilateral V1 lesions experienced conscious perception of phosphenes (brief flashes) via TMS stimulation of the parietal cortex ipsilateral to the lesion. This result is consistent with the visual perception of patient G.S. Given the absence of V1 in these patients, Mazzi's results suggest these feedback signals, and maybe V1 itself, might not play a role in visual awareness (Silvanto, 2014). A similar suggestion comes from a recent study by Ffytche and Zeki (2011). Three hemianopic patients with unilateral lesions to V1 detected, with a performance above chance, visual stimuli moving in different directions and presented at several contrast levels within their blind field. The study of Ffytche and Zeki reinforces the idea that primary visual cortex or back-projections to it are not needed for visual awareness. The discrepancy with previous studies may be explained considering the repeated testing over decades of some patients like G.Y. (Barbur et al., 1993; Zeki and Ffytche, 1998) whose visual pathways might have been consistently modified (Cowey, 2004). Taken together, the present results along with Ffytche and Zeki (2011), and Tinelli et al. (2013) support the view that retinotopically organized activity in V1 is not essential for *conscious* perception, even when the lesion occurs in the developing brain.

## Acknowledgements

This research was funded by the European Research Council FP7-IDEAS-ERC- under the project “Early Sensory Cortex Plasticity and Adaptability in Human Adults – ECSPLAIN” (Grant no. 338866 to M.C.M, K.M.) and the Italian Ministry of University and Research under the project “Futuro in Ricerca” (Grant no. RBFR1332DJ to R.A. and S.C.). We would like to thank Jan W. Kurzawski for his help with DTI analysis. The authors report no competing interest.

## References

Ajina, S., Kennard, C., Rees, G., Bridge, H., 2015a. Motion area V5/MT+ response to global motion in the absence of V1 resembles early visual cortex. Brain 138, 164–178.

Ajina, S., Pestilli, F., Rokem, A., Kennard, C., Bridge, H., 2015b. Human blindsight is mediated by an intact geniculo-extrastriate pathway. eLife 4.

Alais, D., Blake, R., 2005. Binocular Rivalry. MIT Press, Cambridge, Massachusetts, London, England.

Amicuzi, I., Stortini, M., Petrarca, M., Di Giulio, P., Di Rosa, G., Fariello, G., Longo, D., Cannata, V., Genovese, E., Castelli, E., 2006. Visual recognition and visually guided action after early bilateral lesion of occipital cortex: a behavioral study of a 4.6-year-old girl. Neurocase 12, 263–279.

Atkinson, J., 2017. The Davida Teller Award Lecture, 2016: visual brain development: a review of "Dorsal Stream Vulnerability"-motion, mathematics, amblyopia, actions, and attention. J. Vis. 17, 26.

Barbur, J.L., Watson, J.D., Frackowiak, R.S., Zeki, S., 1993. Conscious visual perception without V1. Brain 116 (Pt 6), 1293–1302.

Battista, J., Kalloniatis, M., Metha, A., 2005. Visual function: the problem with eccentricity. Clin. Exp. Optom. 88, 313–321.

Behrens, T.E.J., Johansen-Berg, H., Woolrich, M.W., Smith, S.M., Wheeler-Kingshott, C.A.M., Boulby, P.A., Barker, G.J., Sillery, E.L., Sheehan, K., Ciccarelli, O., Thompson, A.J., Brady, J.M., Matthews, P.M., 2003. Non-invasive mapping of connections between human thalamus and cortex using diffusion imaging. Nat. Neurosci. 6, 750–757.

Berker, E.A., Berker, A.H., Smith, A., 1986. Translation of Broca's 1865 report. Localization of speech in the third left frontal convolution. Arch. Neurol. 43, 1065–1072.

Berlucchi, G. (2017). Wandering thoughts about consciousness, the brain, and the commentary system of Larry Weiskrantz. Neuropsychologia. https://doi.org/10.1016/j.neuropsychologia.2017.10.011.

Biagi, L., Crespi, S.A., Tosetti, M., Morrone, M.C., 2015. BOLD response selective to flow-motion in very young infants. PLoS Biol. 13, e1002260.

Bittar, R.G., Ptito, M., Faubert, J., Dumoulin, S.O., Ptito, A., 1999. Activation of the remaining hemisphere following stimulation of the blind hemifield in hemispherectomized subjects. NeuroImage 10, 339–346.

Bourne, J.A., Morrone, M.C., 2017. Plasticity of visual pathways and function in the developing brain: is the Pulvinar a Crucial Player? Front. Syst. Neurosci. 11.

Bourne, J.A., Rosa, M.G., 2006. Hierarchical development of the primate visual cortex, as revealed by neurofilament immunoreactivity: early maturation of the middle temporal area (MT). Cereb. Cortex 16, 405–414.

Brainard, D.H., 1997. The psychophysics toolbox. Spat. Vis. 10, 433–436.

Bridge, H., Thomas, O., Jbabdi, S., Cowey, A., 2008. Changes in connectivity after visual cortical brain damage underlie altered visual function. Brain 131, 1433–1444.

Bullier, J., 2001. Integrated model of visual processing. Brain Res. Rev. 36, 96–107.

Cardin, V., Smith, A.T., 2010. Sensitivity of human visual and vestibular cortical regions to egomotion-compatible visual stimulation. Cereb. Cortex 20, 1964–1973 (New York, N.Y. : 1991).

Carr, L.J., Harrison, L.M., Evans, A.L., Stephens, J.A., 1993. Patterns of central motor reorganization in hemiplegic cerebral palsy. Brain 116 (Pt 5), 1223–1247.

Corthout, E., Uttl, B., Walsh, V., Hallett, M., Cowey, A., 1999. Timing of activity in early visual cortex as revealed by transcranial magnetic stimulation. Neuroreport 10, 2631–2634.

Cowey, A., 2004. The 30th Sir Frederick Bartlett lecture: fact, artefact, and myth about blindsight. Q. J. Exp. Psychol. Sect. a-Human. Exp. Psychol. 57, 577–609.

Cowey, A., 2010. Visual system: how does blindsight arise? Curr. Biol. 20, R702–R704.

Cowey, A., Stoerig, P., 1991. The neurobiology of blindsight. Trends Neurosci. 14, 140–145.

Cowey, A., Stoerig, P., Bannister, M., 1994. Retinal ganglion-cells labeled from the pulvinar nucleus in Macaque monkeys. Neuroscience 61, 691–705.

Crick, F., Koch, C., 1995. Are we aware of neural activity in primary visual-cortex. Nature 375, 121–123.

Dumoulin, S.O., Wandell, B.A., 2008. Population receptive field estimates in human visual cortex. NeuroImage 39, 647–660.

Engel, S.A., Glover, G.H., Wandell, B.A., 1997. Retinotopic organization in human visual cortex and the spatial precision of functional MRI. Cereb. Cortex 7, 181–192.

Ffytche, D.H., Zeki, S., 2011. The primary visual cortex, and feedback to it, are not necessary for conscious vision. Brain 134, 247–257.

Galantucci, S., Tartaglia, M.C., Wilson, S.M., Henry, M.L., Filippi, M., Agosta, F., Dronkers, N.F., Henry, R.G., Ogar, J.M., Miller, B.L., Gorno-Tempini, M.L., 2011. White matter damage in primary progressive aphasias: a diffusion tensor tractography study. Brain 134, 3011–3029.

Giaschi, D., Jan, J.E., Bjornson, B., Young, S.A., Tata, M., Lyons, C.J., Good, W.V., Wong, P.K.H., 2003. Conscious visual abilities in a patient with early bilateral occipital damage. Dev. Med. Child Neurol. 45, 772–781.

Greco, V., Frijia, F., Mikellidou, K., Montanaro, D., Farini, A., D'Uva, M., Poggi, P., Pucci, M., Sordini, A., Morrone, M.C., Burr, D.C., 2016. A low-cost and versatile system for projecting wide-field visual stimuli within fMRI scanners. Behav. Res. Methods 48, 614–620.

Guzzetta, A., D'Acunto, G., Rose, S., Tinelli, F., Boyd, R., Cioni, G., 2010. Plasticity of the visual system after early brain damage. Dev. Med. Child Neurol. 52, 891–900.

Huk, A.C., Dougherty, R.F., Heeger, D.J., 2002. Retinotopy and functional subdivision of human areas MT and MST. J. Neurosci. 22, 7195–7205.

Jenkinson, M., Beckmann, C.F., Behrens, T.E., Woolrich, M.W., Smith, S.M., 2012. FSL. NeuroImage 62, 782–790.

Johansen-Berg, H., Behrens, T.E., Robson, M.D., Drobnjak, I., Rushworth, M.F., Brady, J.M., Smith, S.M., Higham, D.J., Matthews, P.M., 2004. Changes in connectivity profiles define functionally distinct regions in human medial frontal cortex. Proc. Natl. Acad. Sci. USA 101, 13335–13340.

Kiper, D.C., Zesiger, P., Maeder, P., Deonna, T., Innocenti, G.M., 2002. Vision after early-onset lesions of the occipital cortex: I. Neuropsychological and psychophysical

studies. Neural Plast. 9, 1–25.
Kleiner, M., Brainard, D., Pelli, D., Ingling, A., Murray, R., Broussard, C., 2007. What's new in Psychtoolbox-3. Perception 36 (1-1).
Kuhnke, N., Juenger, H., Walther, M., Berweck, S., Mall, V., Staudt, M., 2008. Do patients with congenital hemiparesis and ipsilateral corticospinal projections respond differently to constraint-induced movement therapy? Dev. Med. Child Neurol. 50, 898–903.
Lamme, V.A.F., Roelfsema, P.R., 2000. The distinct modes of vision offered by feedforward and recurrent processing. Trends Neurosci. 23, 571–579.
Levelt, W.J. (1965). On Binocular Rivalry. Netherlands.
Lunghi, C., Binda, P., Morrone, M.C., 2010. Touch disambiguates rivalrous perception at early stages of visual analysis. Curr. Biol. 20, R143–R144.
Malikovic, A., Amunts, K., Schleicher, A., Mohlberg, H., Eickhoff, S.B., Wilms, M., Palomero-Gallagher, N., Armstrong, E., Zilles, K., 2007. Cytoarchitectonic analysis of the human extrastriate cortex in the region of V5/MT+: a probabilistic, stereotaxic map of area hOc5. Cereb. Cortex 17, 562–574.
Mazzi, C., Mancini, F., Savazzi, S., 2014. Can IPS reach visual awareness without V1? Evidence from TMS in healthy subjects and hemianopic patients. Neuropsychologia 64, 134–144.
Mikellidou, K., Kurzawski, J.W., Frijia, F., Montanaro, D., Greco, V., Morrone, M.C., Burr, D.C., 2017. Area Prostriata in the human brain. Curr. Biol. 27, 3056–3060.
Morrone, M.C., Tosetti, M., Montanaro, D., Fiorentini, A., Cioni, G., Burr, D.C., 2000. A cortical area that responds specifically to optic flow, revealed by fMRI. Nat. Neurosci. 3, 1322–1328.
Muckli, L., Naumer, M.J., Singer, W., 2009. Bilateral visual field maps in a patient with only one hemisphere. Proc. Natl. Acad. Sci. USA 106, 13034–13039.
Nakagawa, S., Tanaka, S., 1984. Retinal projections to the pulvinar nucleus of the macaque monkey: a re-investigation using autoradiography. Exp. Brain Res. 57, 151–157.
Passingham, R.E., Lau, H.C., 2017. Acting, seeing, and conscious awareness. Neuropsychologia.
Pitzalis, S., Sereno, M.I., Committeri, G., Fattori, P., Galati, G., Patria, F., Galletti, C., 2010. Humanv6: the medial motion area. Cereb. Cortex 20 (411–424).
Ptito, A., Leh, S.E., 2007. Neural substrates of blindsight after hemispherectomy. Neuroscientist 13, 506–518.
Rees, G., Kreiman, G., Koch, C., 2002. Neural correlates of consciousness in humans. Nat. Rev. Neurosci. 3, 261–270.
Sanchez-Lopez, J., Pedersini, C.A., Di Russo, F., Cardobi, N., Fonte, C., Varalta, V., Prior, M., Smania, N., Savazzi, S., Marzi, C.A., 2017. Visually evoked responses from the blind field of hemianopic patients. Neuropsychologia. http://dx.doi.org/10.1016/j.neuropsychologia.2017.10.008.
Sereno, M., Dale, A., Reppas, J., Kwong, K., Belliveau, J., Brady, T., Rosen, B., Tootell, R., 1995. Borders of multiple visual areas in humans revealed by functional magnetic resonance imaging. Science 268, 889–893.
Silvanto, J., 2014. Is primary visual cortex necessary for visual awareness? Trends Neurosci. 37, 618–619.
Singh, K.D., Smith, A.T., Greenlee, M.W., 2000. Spatiotemporal frequency and direction sensitivities of human visual areas measured using fMRI. NeuroImage 12, 550–564.
Smith, A.T., Greenlee, M.W., Singh, K.D., Kraemer, F.M., Hennig, J., 1998. The processing of first- and second-order motion in human visual cortex assessed by functional magnetic resonance imaging (fMRI). J. Neurosci.: Off. J. Soc. Neurosci. 18, 3816–3830.
Stoerig, P., Cowey, A., 2007. Blindsight. Curr. Biol. 17, R822–R824.
Tamietto, M., Morrone, M.C., 2016. Visual plasticity: blindsight bridges anatomy and function in the visual system. Curr. Biol. 26, R60–R82.
Tinelli, F., Cicchini, G.M., Arrighi, R., Tosetti, M., Cioni, G., Morrone, M.C., 2013. Blindsight in children with congenital and acquired cerebral lesions. Cortex 49, 1636–1647.
Tong, F., 2003. Primary visual cortex and visual awareness. Nat. Rev.: Neurosci. 4, 219–229.
Tootell, R.B.H., Mendola, J.D., Hadjikhani, N.K., 1997. Functional analysis of V3A and related areas in human visual cortex. J. Neurosci. 17, 7060–7078.
Vernet, M., Japee, S., Lokey, S., Ahmed, S., Zachariou, V., Ungerleider, L.G., 2017. Endogenous visuospatial attention increases visual awareness independent of visual discrimination sensitivity. Neuropsychologia.
Wandell, B., Brewer, A., Dougherty, R.F., 2005. Visual field map clusters in human cortex. Philos. Trans. R. Soc. B: Biol. Sci. 360, 693–707.
Warner, C.E., Goldshmit, Y., Bourne, J.A., 2010. Retinal afferents synapse with relay cells targeting the middle temporal area in the pulvinar and lateral geniculate nuclei. Front. Neuroanat. 4.
Warner, C.E., Kwan, W.C., Bourne, J.A., 2012. The early maturation of visual cortical area MT is dependent on input from the retinorecipient medial portion of the inferior pulvinar. J. Neurosci. 32, 17073–17085.
Warner, C.E., Kwan, W.C., Wright, D., Johnston, L.A., Egan, G.F., Bourne, J.A., 2015. Preservation of vision by the pulvinar following early-life primary visual cortex lesions. Curr. Biol. 25, 424–434.
Weiskrantz, L., 1986. Blindsight: A Case Study and Implications. Oxford University Pres, Oxford.
Weiskrantz, L., Warrington, E.K., Sanders, M.D., Marshall, J., 1974. Visual capacity in the hemianopic field following a restricted occipital ablation. Brain 97, 709–728.
Werth, R., 2006. Visual functions without the occipital lobe or after cerebral hemispherectomy in infancy. Eur. J. Neurosci. 24, 2932–2944.
Werth, R., 2008. Cerebral blindness and plasticity of the visual system in children. A review of visual capacities in patients with occipital lesions, hemispherectomy or hydranencephaly. Restor. Neurol. Neurosci. 26, 377–389.
Wilke, M., Staudt, M., Juenger, H., Grodd, W., Braun, C., Krageloh-Mann, I., 2009. Somatosensory system in two types of motor reorganization in congenital hemiparesis: topography and function. Human. Brain Mapp. 30, 776–788.
Yeatman, J.D., Dougherty, R.F., Myall, N.J., Wandell, B.A., Feldman, H.M., 2012. Tract profiles of white matter properties: automating fiber-tract quantification. PLoS One 7.
Yu, H.H., Chaplin, T.A., Egan, G.W., Reser, D.H., Worthy, K.H., Rosa, M.G., 2013. Visually evoked responses in extrastriate area MT after lesions of striate cortex in early life. J. Neurosci. 33, 12479–12489.
Zeki, S., 1993. A Vision of the Brain. Blackwell Scientific, Oxford.
Zeki, S., Ffytche, D.H., 1998. The Riddoch syndrome: insights into the neurobiology of conscious vision. Brain 121, 25–45.
Zeki, S., Watson, J.D., Lueck, C.J., Friston, K.J., Kennard, C., Frackowiak, R., 1991. A direct demonstration of functional specialization in human visual cortex. J. Neurosci. 11, 641–649.